Dynamics of Benzene Guest Inside a Self-Assembled Cylindrical Capsule: A Combined Solid-State ^{2}H NMR and Molecular Dynamics Simulation Study

Alexandra R. Albunia, Carmine Gaeta, Placido Neri,* Alfonso Grassi,* and Giuseppe Milano

Dipartimento di Chimica, Università di Salerno, Via Ponte don Melillo, I-84084 Fisciano (Salerno), Italy

Received: March 21, 2006; In Final Form: July 21, 2006

The reorientational dynamics of benzene-d_6 molecules hosted into the cavity of a cavitand-based, self-assembled capsule was investigated by Molecular Dynamics (MD) simulations and temperature-dependent solid-state ^{2}H NMR spectroscopy. MD simulations were preliminarily performed to assess the motional models of the guest molecules inside the capsules. An in-plane fast reorientation of the benzene guest around the C_6 symmetry axis (B1 motion), characterized by correlation times of the order of picoseconds, was predicted with an activation barrier (∼8 kJ/mol) very similar to that found for neat benzene in the liquid state. An out-of-plane reorientation corresponding to a nutation of the C_6 symmetry axis in a cone angle of 39° (B2 motion, 373 K) with an activation barrier (∼39 kJ/mol) definitely larger than that of liquid benzene was also anticipated. In the temperature range 293−373 K correlation times of the order of a nanosecond have been calculated and a transition from fast to slow regime in the ^{2}H NMR scale has been predicted between 293 and 173 K. ^{2}H NMR spectroscopic analysis, carried out in the temperature range 173−373 K on the solid capsules containing the perdeuterated guest (two benzene molecules/capsule), confirmed the occurrence of the B1 and B2 motions found in slow exchange in the ^{2}H NMR time scale. Line shape simulation of the ^{2}H NMR spectral lines permitted defining a cone angle value of 39° at 373 K and 35° at 173 K for the nutation axis. The T_1 values measured for the ^{2}H nuclei of the encapsulated aromatic guest gave correlation times and energetic barrier for the in-plane motion B1 in fine agreement with theoretical calculation. The experimental correlation time for B2 as well as the corresponding energetic barrier are in the same range found for B1. A molecular mechanism for the encapsulated guest accounting for the B1 and B2 motions was also provided.

Introduction

In recent years increasing research efforts have been devoted to the construction of self-assembled capsules.[1] Among the possible supramolecular interactions, hydrogen bonding has been largely exploited to drive the self-assembly process.[1] In this way several examples of H-bonded capsules based on glycoluril,[2] calixarene,[3] or the resorcinarene[4] skeleton have been reported.

The interior of these capsules is usually seen as a "special space" in which interesting phenomena can be observed due to the reversible confinement of one, two, or very few guest species from the external bulk solvent molecules.[1] Thus, for example, Rebek et al. have demonstrated that guests encapsulated into the cavitand-based cylindrical capsule **1·1** (Figure 1) are unable to tumble,[5] adopt unusual compacted[6] or helical[7] conformation, discriminate the co-guest by virtue of its dimension[4b,5,8] or chirality,[9] display noncovalent isotope effects,[10] present new forms of supramolecular isomerism,[11] and show a modified reactivity.[5a,12] Most of these properties are strictly related to the size and dynamics of the guest molecules inside the cavity and to the possibility of positional exchange between the inner and outer capsule space.

In particular, it was previously shown that when two benzene molecules are encapsulated in **1·1**, they both tumble freely while for toluene the behavior of the two guest molecules is close to the limit of molecular tumbling.[5a] Increasing the steric bulkiness of the substituents at the aromatic ring, e.g., as in *p*-xylene, produces a rigid orientation of the guest.[5a]

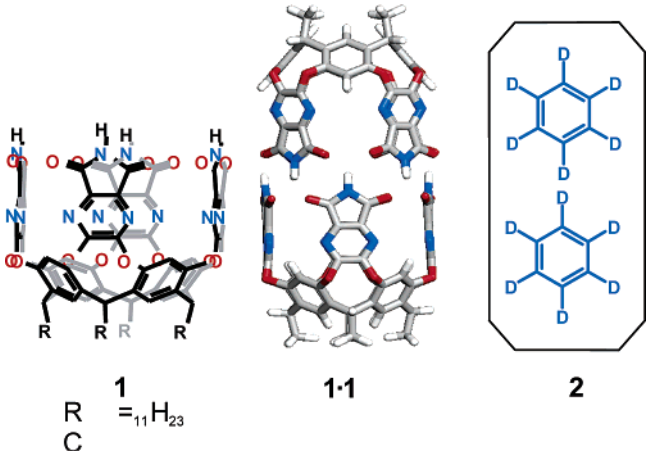

Figure 1. Structure of cavitand **1**, energy-minimized model of the **1·1** dimeric capsule (R groups are omitted for clarity), and schematic representation of guest-filled capsule **2**.

The ^{2}H ($I = 1$) NMR line shape of deuterated organic molecules in the solid state is dominated by nuclear quadrupolar coupling and the frequency spacing between the spectral lines depends on the quadrupole coupling constant of deuterium nuclei Q_0 and the angle between the C−D bond vector and the magnetic field.[13] The quadrupolar interactions are also sensitive to molecular dynamics and the spectral line spacing is dramatically affected by the kind and correlation time τ_C of the motion. Reorientation of the C−D vector in the space is in the so-called fast regime when $\tau_C \ll Q_0^{-1} = 10^{-6}$ s, whereas the molecule is

* Address correspondence to these authors. Phone: +39-089-96-9591. Fax: +39-089-96-9603. E-mail: agrassi@unisa.it and neri@unisa.it.

10.1021/jp0617423 CCC: $33.50
Published on Web 09/13/2006

considered static in the ^{2}H NMR time scale when $\tau_C \gg Q_0^{-1}$. Axially symmetric fast motions produce a line splitting that further depends on the angle between this axis and magnetic field.

Reorientational dynamics of aromatic molecules clathrated in the voids of crystalline organic molecules,[14a−c] polymers,[14d−f] zeolites,[14g] or carcerands[14h,i] has been investigated with this method, providing interesting information on the motions permitted for the guest molecules and on the corresponding host−guest interactions. The ^{2}H NMR analysis of guest-filled solid capsules **1·1** can also provide detailed information on the optimal occupancy of the capsule space and to detect possible stereoisomerism of the encapsulated molecules, ruling out the contribution to the spectral lines resulting from external solvent and in−out capsule exchange phenomena. Moreover, the ^{2}H NMR spectroscopy allows the detection of dynamics operating in a time scale different from that monitored by ^{1}H NMR spectroscopy, already employed in solution NMR investigation of the same compounds.[4b,5−12]

The reorientation of ring molecules in condensed phases has also been investigated by simulation studies. Müller-Plathe reported a molecular dynamics (MD) study on the reorientation anisotropy of benzene molecules in solvent-swollen polymers,[15] and more recently, further studies about the reorientational motion of benzene in the neat liquid and in a polystyrene/benzene solutions by ^{1}H NMR relaxation as well as MD simulation methods.[16]

Aiming to provide a closer insight into the dynamics of aromatic guests inside the H-bonded self-assembled capsule, here we report a combined study of the mobility in the solid state of the encapsulation products of **1·1** with benzene-d_6 (**2**) by ^{2}H NMR spectroscopy and molecular dynamics simulations.

Experimental Section

Materials. All operations were performed under aerobic conditions. Benzene-d_6 (99 atom % D, Aldrich) was used as received. All reagents are reagent-grade quality and were used without further purification. Cavitand **1** was prepared according to the procedure by Rebek et al.[5a]

*Preparation of Benzene-Filled Capsules **2**.* Powder samples of guest-filled capsules were precipitated from solutions of the cavitand **1** (0.40 g) in benzene-d_6 (5 mL) upon addition of *n*-pentane (3 mL) at room temperature. The solid sample was isolated by filtration and dried at room temperature in vacuo (10 Torr; 24 h) to give 0.15 g of powder benzene-filled capsules **2**.

*Determination of Average Guest/Capsule Composition in **2** by Quantitative ^{2}H NMR.* The samples were prepared by dissolving 20 mg of powder guest-filled capsules **2** in acetone (0.4 mL) containing 70 μL of acetone-d_6 (0.28 M) as internal standard. The guest/capsule stoichiometry was evaluated by integration of the ^{2}H NMR signals of acetone-d_6 vs the aromatic deuterons of the guest molecules. The value found of 1.7 benzene-d_6 molecules/capsule is in satisfactory agreement with the value of 2 found by Rebek et al. for the analogue complex prepared and analyzed in situ in mesitylene solution.[4b,5a] The slight discrepancy can be attributed to a small fraction of noninteger capsules produced during the synthetic procedure.

Computational Details. Molecular dynamics (MD) simulations have been carried out with the YASP suite of programs.[17] MD was run at constant temperature *T* and constant volume *V*, by weak coupling[18] to a temperature bath of the appropriate target temperature (see below). The coupling time was 0.2 ps (*T*). The time step was 2 fs. Carbon−hydrogen bond lengths were constrained by using the SHAKE[19] algorithm. Models reproducing the amorphous phase of cavitands have been considered. A cubic box containing four self-assembled capsules **1·1** placed in a random orientation, each one bearing two guest molecules per cavity, has been modeled. In the NVT simulations in periodic boundary conditions the box length has been fixed to 3.37 nm. This corresponds to a density of ~0.61 g/cm^3 that is about 70−80% of the density of crystals of similar inclusion compounds.[20] The force field parameters for the capsules were derived from the OPLS force field.[21]

SCHEME 1: Atom Labeling and Orientation Vectors for Benzene

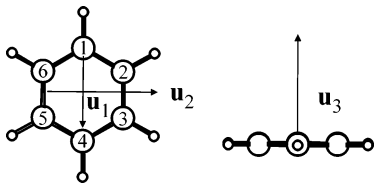

For benzene, the nonbonded parameters of Jorgensen and Severance[21] have been adjusted to reproduce the experimental density (at 1 atm) and the heat of vaporization of liquid benzene. With this benzene force field, different properties such as diffusion coefficients and the reorientational motion of benzene in the neat liquid and in polystyrene−benzene solutions, structure, and thermodynamics of cyclohexane−benzene mixtures have been successfully calculated by previous molecular dynamics simulations.[15,16,22]

The rotation of a benzene molecule can be characterized by the time evolution of certain molecule-fixed unit vectors. They are illustrated in Scheme 1. We arbitrarily take as unit vector $\mathbf{u}_1$ the in-plane vector from C_1 in the direction of C_4. The other in-plane vector $\mathbf{u}_2$, which is perpendicular to $\mathbf{u}_1$, is symmetrically equivalent ($\mathbf{u}_1$ and $\mathbf{u}_2$ together form a degenerate representation of the molecular point group) and contains no new information. A third orientation vector $\mathbf{u}_3$ is given by the ring normal **n**. This was calculate as the appropriately normalized arithmetic mean of the normals of the two planes defined by atoms C_1, C_3, and C_5 and C_2, C_4, and C_6, respectively.

In the following, to characterize the in-plane and out-of-plane reorientation processes, we will refer to $\mathbf{u}_2$ as $\mathbf{u}_{||}$ and to $\mathbf{u}_3$ as $\mathbf{u}_\perp$.

Techniques. *^{2}H NMR Spectroscopy.* Solution high-resolution ^{2}H NMR spectra were collected on a Bruker Avance 400 (61.4 MHz for ^{2}H Larmor frequency) with a pulse width of 10 μs (90°) and a recycle time of 2 s to ensure quantitative analysis.

Solid-state ^{2}H NMR measurements were performed on a Bruker Avance 300 (46.07 MHz for ^{2}H Larmor frequency) with a 10 mm sample tube. The spectra were acquired by using a solid echo pulse sequence ($90°_x-\tau_1-90°_y-\tau_2-$ACQ), with echo delay τ_1 of 50 μs and τ_2 of 45 μs. The ^{2}H spin−lattice relaxation times T_1 were measured by using a three-pulse inversion−recovery−echo sequence ($180°_x-t_3-90°_x-t_1-90°_y-t_2-$ACQ) with time increments t_3 varied from 1 to 500 ms. The T_1 values of Table 5 are average values of at least six measurements. Pulse length of 90° (5.7 μs) and a recycle time 1 s were used to ensure quantitative detection. The left shift was carefully chosen so that the first point of the free induction decay (FID) was digitized at the echo maximum. For a typical solid-state ^{2}H NMR spectrum 10 K transients were accumulated.

The line shape analysis of 1D solid echo spectra has been performed with the NMR-WEBLAB program.[23] The anisotropy parameter $\delta Q = {}^3/_4(e^2Qq/h)$ equal to 137 kHz has been set for the aromatic deuterons in the spectral line shape simulation.

SCHEME 2: The Two Kind of Motions Simulated: Fast In-plane Rotation about the C_6 Axis (motion B1), and Fast Precessional Motion (nutation) of the C_6 Axis in a Cone of Angle θ (motion B2)

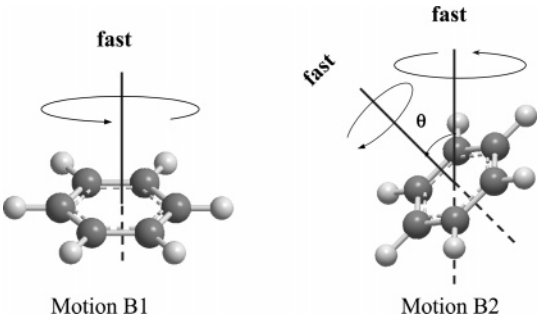

TABLE 1: Simulation Conditions for the Systems I−V of 2

system	T [K]	simulation time [ps]
I	173	12000
II	293	10546
III	300	5880
IV	330	4600
V	373	5000

Two kinds of motion, pictured in Scheme 2**,** were simulated: (i) fast in-plane rotation about the C_6 axis (motion B1)and (ii) fast precessional motion (nutation) of the C_6 axis in a cone of angle θ (motion B2).

Infrared Spectroscopy (*FT-IR*). FT-IR spectra were obtained at a resolution of 2.0 cm^{-1} with a Bruker Vector 22 spectrometer equipped with deuterated triglycine sulfate (DTGS) detector and a Ge/KBr beam splitter. The frequency scale was internally calibrated with a He−Ne laser. A total of 32 scans were acquired for each spectrum to increase the signal/noise ratio.

Thermogravimetry. The thermogravimetric analysis (TGA) was carried out with a Mettler TG50 thermobalance in flowing nitrogen atmosphere, using 10 mg of sample and a heating rate of 10 deg/min.

Results and Discussion

Molecular Dynamics Simulations. Models for the amorphous phase of the encapsulation product of **1·1** with benzene-d_6 (**2**) have been simulated in the temperature range 173−373 K (Systems I−V; Table 1) by all-atom Molecular Dynamics (MD) simulations. A snapshot of one of the four cavitand host/guest complexes of System II, after 2 ns of simulation, has been sketched in Figure 2. In the considered temperature range of 173−373 K, the capsules undergo a small bending of the walls (i.e., the dichloropyrazine-2,3-dicarboxylic acid imide moieties) with an occasional reduction of the number of hydrogen bonds, while the other main geometrical features are retained during the simulation. In addition, as is expected for a glassy system, fluctuations of capsule geometrical parameters around the equilibrium position are observed.

The reorientation of the benzene guest molecules hosted in the capsule was thus followed by using the unit vectors $\mathbf{u}_{||}$ and $\mathbf{u}_{\perp}$, as defined in the computational details section and shown in Scheme 1. The former vector ($\mathbf{u}_{||}$) probes the in-plane molecular reorientation about the C_6 symmetry axis, while the latter ($\mathbf{u}_{\perp}$) probes the flip motion of the ring plane, or the out-of-plane motion.

The distributions of the reorientation angle ϕ traced by $\mathbf{u}_{||}$ at 173 (System I), 293 (System II) and 373 K (System V) for benzene have been reported in Figure 3. The calculated distributions at room and higher temperature are very flat,

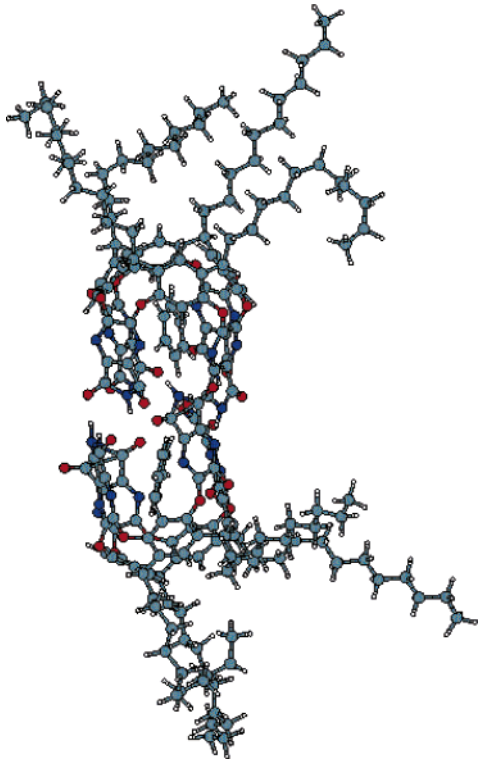

Figure 2. Snapshot of one of the four guest-filled self-assembled capsules present in the simulation cell. The structure corresponds to System II of Table 1 after 2 ns of simulation.

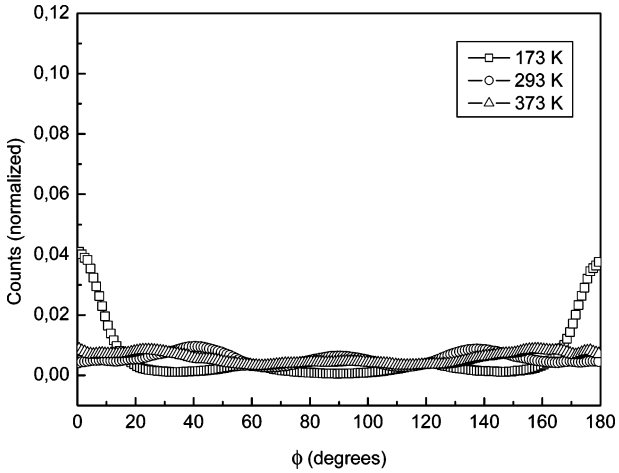

Figure 3. Distributions of the reorientation angle $\phi = \arccos(\mathbf{u}_{||}(t)\cdot\mathbf{u}_{||}(0))$ (plane parallel) at different temperatures for benzene guest molecules.

suggesting that the benzene ring easily gives complete reorientation about the C_6 axis during the simulation time. The reorientation angle ϕ traced by the unit vector $\mathbf{u}_{\perp}$ at 173 (System I), 293 (System II), and 373 K (System V) has been sketched in Figure 4. The hystograms at the lowest temperature indicate that in the simulation time scale (nanoseconds) the motion is restricted. This is only a limitation of the computational approach used and no evidence of restricted rotation has been found experimentally.

From the calculated distributions at a given temperature, and, in particular, by intersecting the corresponding Boltzmann inverted distribution at a value of $\sim kT$, it is possible to estimate the maximum $\mathbf{u}_{\perp}$ reorientation angle. Values of ϕ_{max} of 32° and 39° can be estimated for the systems at 293 and 373 K, respectively.

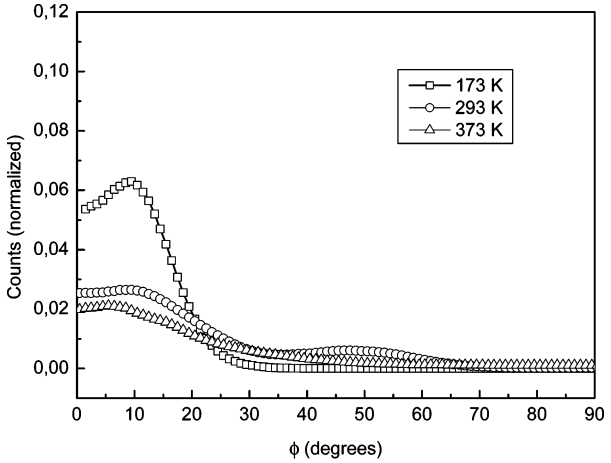

Figure 4. Distributions of the reorientation angle $\phi = \arccos(\mathbf{u}_\perp(t)\cdot\mathbf{u}_\perp(0))$ (plane perpendicular) at different temperatures for benzene guests molecules.

TABLE 2: Benzene Reorientation Times[a] for $\mathbf{u}_1$ ($\mathbf{u}_\parallel$) and $\mathbf{u}_3$ ($\mathbf{u}_\perp$) Vectors Calculated from MD Trajectories

T [K]	$\tau_\parallel$ [ps]	$\tau_\perp$ [ns]
173	80 ± 10	$\sim 2 \times 10^6$ [b]
293	9 ± 3	28 ± 3
300	7 ± 4	26 ± 8
330	5.0 ± 0.8	5.80 ± 0.03
373	2 ± 1	0.6 ± 0.1

[a] Calculated from eq 3. [b] Calculated from eq 4.

As already reported by Müller-Plathe,[15,16] the in-plane and out-of-plane reorientational dynamics of a planar molecule can be quantitatively characterized considering the decay of the corresponding time correlation function

$$\langle \cos\phi \rangle = \langle \mathbf{u}(t)\cdot\mathbf{u}(0) \rangle \tag{1}$$

This correlation function describes by what angle, on average, $\mathbf{u}$ has rotated at time t, given that it was in position $\mathbf{u}(0)$ at time $t = 0$. Ensemble averaging is accomplished through averaging over both molecules and time origins. For molecular liquids, these correlation functions are often found to follow an exponential decay after some short-time features. These correlation functions can be fitted by stretched-exponential or Kohlrausch−Williams−Watts (KWW) functions

$$\langle \mathbf{u}(t)\cdot\mathbf{u}(0) \rangle \approx \exp\left[-\left(\frac{t}{\alpha}\right)^\beta\right] \tag{2}$$

A correlation time characteristic of the particular reorientation can be calculated as the time integral of the correlation function, which in the case of a stretched exponential can be expressed with the Euler Γ function:

$$\tau = \int_0^\infty \exp\left(-\left(\frac{t}{\alpha}\right)^\beta\right) \mathrm{d}t = \frac{\alpha}{\beta}\Gamma\left(\frac{1}{\beta}\right) \tag{3}$$

The correlation times corresponding to the motions leading to reorientation of $\mathbf{u}_\parallel$ and $\mathbf{u}_\perp$ have also been denoted as $\tau_\parallel$ and $\tau_\perp$, respectively.

As reported in Table 2, the calculated values of $\tau_\parallel$ for an encapsulated benzene molecule go from 2 ± 1 ps for the system simulated at 373 K to 80 ± 10 ps for the system simulated at 173 K.

The reorientation is a thermally activated process and thus an Arrhenius equation is often valid in describing the temperature dependence of the correlation times

$$\tau = \tau_0 \exp\left(\frac{E_A}{RT}\right) \tag{4}$$

By fitting the behavior of the correlation times $\tau_\parallel$ calculated at different temperatures it is possible to obtain an activation energy for the in-plane reorientation process. In Figure 5a is reported the Arrhenius-like plot of $\ln\tau_\parallel$ vs $1/T$. The value of $\sim$8 kJ/mol of activation energy obtained by the fitting (see Table 3) is similar to the one obtained by Müller-Plathe and co-workers (7 kJ/mol) for liquid benzene[16] and thus suggests that encapsulation of the benzene molecule in the cavitand **1·1** does not affect significantly the in-plane reorientation.

In Figure 5b is reported the Arrhenius-like plot of $\ln\tau$ vs $1/T$. In this case the calculated of activation energy of $\sim$40 kJ/mol is almost four times the value reported for liquid benzene.[15,16]

The calculated values of $\tau_\perp$ for benzene go from 0.6 ± 0.1 ns for the system simulated at 373 K to 28 ± 3 ns for the system simulated at 293 K.

For the lowest temperature of 173 K, the decay of the angle autocorrelation function does not go below 0.92 along the entire simulation time of about 12 ns and the reorientation time cannot be evaluated. In this case, the reorientation time has been evaluated by using the eq 4. From the values of τ_0 and E_A obtained by fitting the four values of $\tau_\perp$ in the interval temperature 293−373 K a value of $\tau_\perp$ of $\sim$2000 μs at 173 K can be extrapolated.

To understand the molecular mechanism of the guest reorientation, further geometrical analysis was carried out on each half capsule containing one guest benzene molecule. The distances $D1$ and $D2$ between the geometric centers of the two opposite five-membered imido rings (Figure 6) have been monitored for each system (I−V). In panels a and b of Figure 7 the values of $D1$ and $D2$ for two-half caspules extracted from the simulation at 173 K are plotted as a function of time. From the figures it is clear that in one-half capsule both the distances $D1$ and $D2$ oscillate around a value of about 0.9 nm (Figure 7a), while in the other half capsule $D1$ and $D2$ assume average values of about 0.7 and 1.0 nm, respectively. In Figure 7c we have reported the values of $D1$ and $D2$ for one-half capsule at 330 K. In this case, $D1$ and $D2$ exhibit a sharp complementary behavior in the same half capsule: when $D1$ assumes the value of 0.7 nm, $D2$ shows correspondingly a value of 1 nm and vice versa. This behavior, as sketched in Figure 6, is related to the alternate inclination of each of the four walls present in one-half capsule. In Figure 7d the angle θ between the vector $\mathbf{u}_\perp$ perpendicular to the benzene plane and the $D2$ direction extracted from the 4.6 ns of simulation at 330 K (System IV) is reported as a function of time. On inspection of this figure it can be seen that the θ angle flips among the average values of 30°, 150°, and 90°, corresponding to the possible orientations of the benzene plane always parallel to each inclined wall.

Thus, two possible states of the cavitand, indicated as S1 and S2 in Figure 6, can be identified. In the less frequent state S2, $D1$ and $D2$ exhibit the same value of about 1 nm leading to a symmetric capsule. On the contrary, in state S1, one of the walls is inward to give a shorter distance of about 0.7 nm, while the remaining three retain perpendicular orientation producing a value of 1 nm for $D2$. In this instance, the guest benzene plane is always parallel to the inclined five-membered imido ring and in-plane reorientation is allowed with an eventual wobbling of the benzene ring in a small cone angle. In the symmetrical state S2 an out-of-plane reorientation becomes possible due to the wider space available for the benzene wobbling in a larger cone angle. The exchange rate between states S1 and S2 appears to be beyond the time scale limit of the current MD simulations.

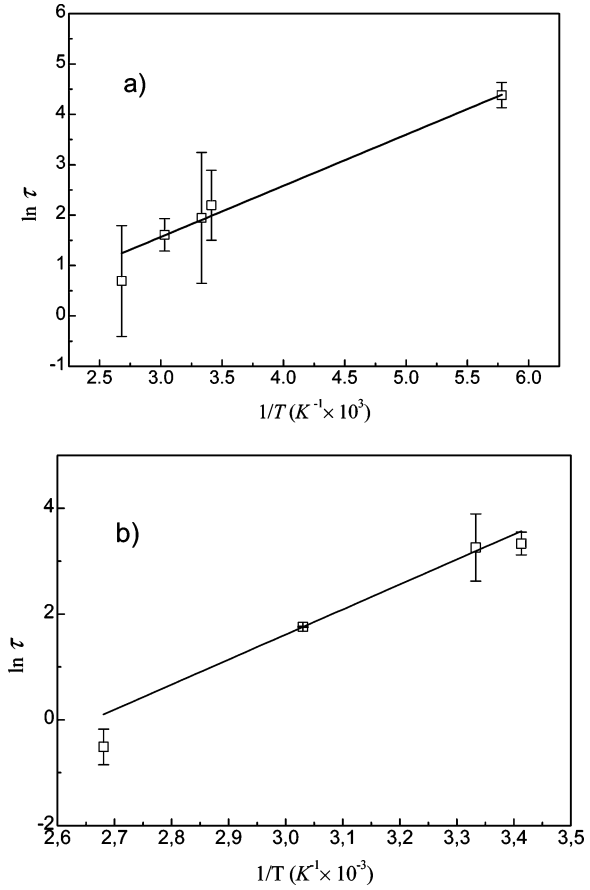

Figure 5. (a) Arrhenius-like log plot for the in-plane reorientation of benzene in **2** (time units ps). (b) Arrhenius-like log plot for the out-of-plane reorientation of benzene in **2** (time units ns).

TABLE 3: Activation Energies by MD Calculations for the In-Plane and Out-of-Plane Reorientation

	benzene	
	as guest	liquid phase[16]
$Ea_{\|\|}$ [kJ/mol]	8.4 ± 0.4	7.1
$Ea_{\perp}$ [kJ/mol]	39 ± 6	9.2

It is interesting to observe that in a entire self-assembled capsule all the combinations of states S1 and S2 are possible leading to symmetrical and asymmetrical capsules: the statistical distribution or the population of these states is related to the free energy difference of the host−guest complexes.

^{2}H NMR Spectra. The experimental solid-state ^{2}H NMR powder spectra of encapsulation products of **1·1** with benzene-d_6 (**2**), in the temperature range 173−373 K, are shown in Figure 8a−c.

The room temperature ^{2}H NMR spectrum exhibits at least two superimposed and not well resolved Pake patterns, corresponding to different reorientational motions, since the largest experimental quadrupolar splitting is narrower than expected for static aromatic deuterons (137 kHz).

The solid-state ^{2}H NMR spectrum of **2** at 173 K (Figure 8a) is very simple and mainly consists of a single ^{2}H Pake pattern with a quadrupolar splitting $\Delta\nu_Q$ of 67 kHz, the same splitting found for solid benzene at 173 K[13] or benzene molecules clathrated in the voids of δ-form of crystalline syndiotactic polystyrene,[14d,e] polycyano-polycadmates,[14c] or zeolite ZSM-5[14g] under comparable conditions. This $\Delta\nu_Q$ value usually has been attributed to the fast in-plane rotation of the molecule about the C_6-symmetry axis (Scheme 2, B1), which reduces the quadrupolar splitting by a factor of about 2 compared to the static value of 137 kHz.[14j] When the temperature is increased, this quadrupolar splitting becomes narrower and assumes the values of 64 kHz at 293 K and 61 kHz at 373 K (Table 4). This temperature-dependent narrowing of a few kilohertz suggests a higher mobility of the molecule in the cavity, which combines the axially symmetric motion B1 (Scheme 2) with a thermally activated wobbling of the benzene ring in a small cone angle.[14j]

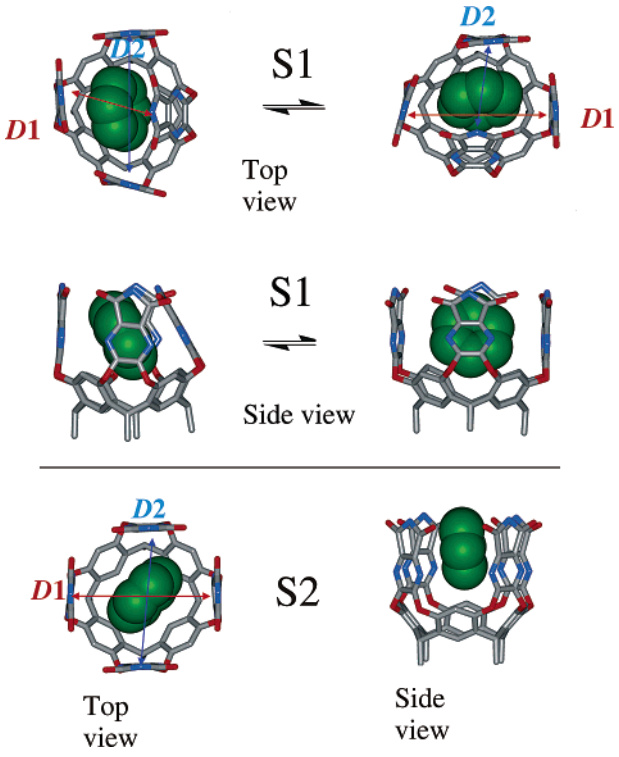

Figure 6. Sketches of the S1 (top) and S2 (bottom) states of a half capsule containing one benzene guest molecule.

As the temperature is increased, an additional broad inner ^{2}H NMR pattern appears in the experimental spectrum (Figure 8b) that is hardly distinguishable at 173 K, but whose intensity increases with temperature to become the main detectable signal at 373 K. However, the corresponding splitting does not change significantly with the temperature (26 kHz at 293 K and 25.4 kHz at 173 K, Table 4). The origin of this ^{2}H NMR pattern is not immediate and requires appropriate line shape simulation (vide infra for details). Finally, in the temperature range 293−373 K a narrow ^{2}H NMR signal at $\nu = 0$ is also detected. However, drying of **2** in high vacuum at room temperature actually reduces significantly the intensity of this signal, leaving the other patterns unchanged. Thus we propose that this signal stems from molecules located outside the capsule or sorbed on its surface and is attributed, on the basis of the line width of 3 kHz, to benzene molecules involved in fast isotropic reorientation. The area of this ^{2}H signal corresponds to about 2 mol % of total benzene and was considered, in first approximation, negligible.

The presence of two independent patterns suggests that there are at least two types of motions that do not exchange rapidly with each other in the ^{2}H NMR time scale.

The ^{2}H NMR line shape analysis was thus carried out by computer simulation on the basis of the MD calculations reported in the previous section and assuming that the reorientation of the guest molecule is in the fast regime region. Superimposing of the fast in-plane rotation of the molecule about the C_6-symmetry axis (Scheme 2, B1) and an out-of-plane

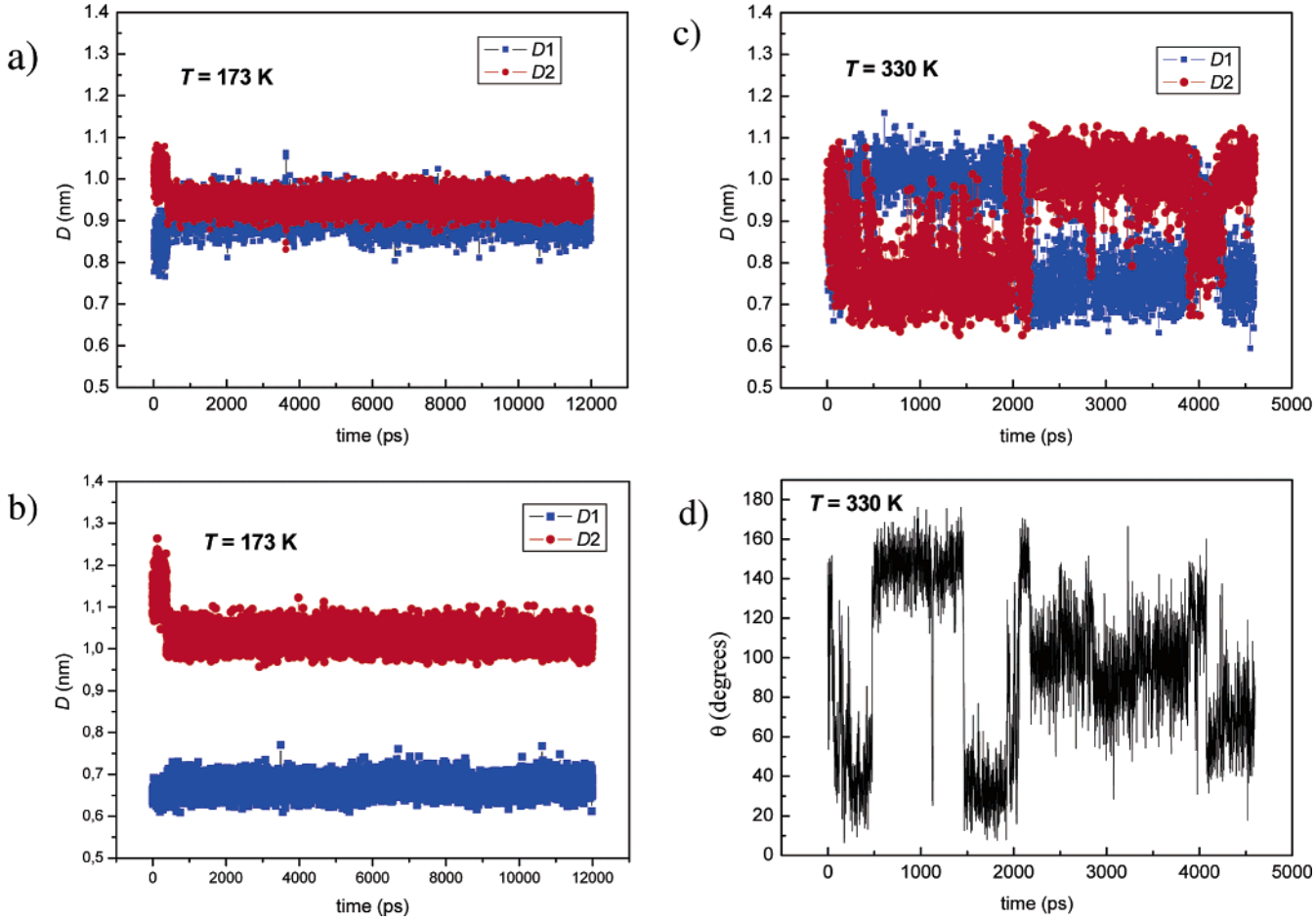

Figure 7. Plot of distances *D*1 and *D*2 as a function of simulation time (a) and (b) at 173 (c) and 330 K. (d) Plot of the angle θ between the vector $\mathbf{u}_\perp$ perpendicular to the benzene plane and the *D*2 direction extracted from the simulation at 330 K (corresponding to Figure 7c) as a function of the simulation time.

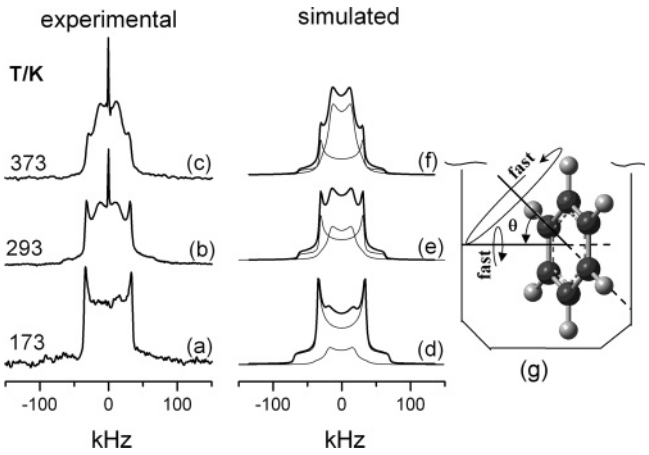

Figure 8. Experimental (a−c) and simulated (d−f) ^{2}H NMR powder spectra of **2** in the temperature range 173−373 K. Each simulated spectrum (thick line) is the sum of two patterns (thin lines) accounting for the in-plane rotation and precessional motion (nutation) of the C_6 asymmetry axis with an angle of 35° (d) and 39° (e and f). (g) Sketch displaying the precession motion of the aromatic guest about the C_6 axis in a cone ϕ.

motion (Scheme 2, B2) at variable values of the nutation of the C_6-axis angle on the surface of a cone with half cone angle θ was thus considered. The best fitting of data gave the θ values of 35° at 173 kHz and 39° at 293 and 373 kHz, respectively (see Table 4 and Figure 8). Simulations carried out assuming fast jumping of the C_6 axis in a solid cone of the same amplitude[14j] gave worse results. In Figure 8d−f the experimental and simulated spectra[23] are compared and the reorientational dynamics of the guest in the capsule is displayed in Figure 8g. As expected the cone angle value becomes smaller as the temperature decreased, reaching the minimum value of 35° at 173 K. The agreement between the MD calculations and simulation of the ^{2}H NMR spectra of solid capsule **2** is

TABLE 4: Experimental $\Delta\nu_Q$ Values and Parameters Used for the Simulation of the ^{2}H NMR Spectral Line Shape of 2 at Different Temperatures

T [K]	$\Delta\nu_Q$ [kHz]	type of motion	simulation parameters[a]	$x_{wobb(nut)}$[b]
373	61	in-plane rotation	$\theta = 90°$ 6 sites, $\psi = 60°$	0.65
	25.4	nutation	$\theta = 39°$ free	
293	64	in-plane rotation	$\theta = 90°$ 6 sites, $\psi = 60°$	0.43
	26	nutation	$\theta = 39°$ free	
173	67	in-plane rotation	$\theta = 90°$ 6 sites, $\psi = 60°$	0.19
	34	nutation	$\theta = 35°$ free	

[a] The NMR-WEBLAB[23] program simulates spectra from molecules with C−D bonds moving on a cone of angle θ in the fast motional limit or in the general case. The geometry of the motion is either characterized by discrete jumps (2-, 3-, 4-, and 6-fold) defined by a flip angle ψ or by a free rotation on a single cone. [b] x_{nut} was evaluated as the ratio $area_{nutation}/(area_{nutation} + area_{in-plane})$.

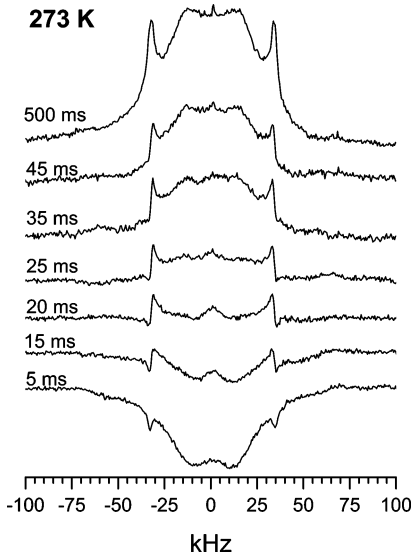

Figure 9. ^{2}H NMR spectra of sample **2** recorded at 273 K using the three-pulse inversion recovery sequence ($180°_x-t_3-90°_x-t_1-90°_y-t_2-$ACQ). On the left side are given the t_3 values in milliseconds (ms).

TABLE 5: T_1 and τ_C Experimental Values of the Guest in 2 Evaluated from the ^{2}H NMR Spectral Analysis

	in-plane rotation (B1)		out-of-plane motion (B2)	
T [K]	T_1 [ms]	τ_c [ps]	T_1 [ms]	τ_c [ps]
233	17	110	20	100
273	27	74	35	58
298	42	48	62	32
323	65	31	110	19

straightforward at 373 K: the discrepancy between the cone angle amplitude at 293 K [$\theta = 39°$ (exptl) vs 32° (calcd)] is likely due to the experimental error of the methods employed.

To compare the correlation time τ_C associated with the B1 and B2 motions, the longitudinal relaxation times T_1 were measured in the temperature range of 253−333 K, using the three-pulse inversion−recovery−echo sequence ($180°_x-t_3-90°_x-t_1-90°_y-t_2-$ACQ) in which the time interval t_3 was varied from 1 to 500 ms (Figure 9). The T_1 values were estimated by using the approximate solution[24] $T_1 = 1.44t_0$, where t_0 is the t_3 value corresponding to the disappearance of the ^{2}H signals in the spectrum. Assuming that the relaxation mechanism is mainly due to the fluctuation of the ^{2}H quadrupole interaction caused by the molecular motions, the theory relates T_1 to the rotational correlation time τ_C of the electric field gradient experienced by the nucleus according to eq 5[25]

$$T_1^{-1} = \frac{3}{40}\frac{(2\pi\Delta e^2Qq)^2}{h}\left(1+\frac{\eta^2}{3}\right)\left[\frac{\tau_C}{1+(\omega_D\tau_C)^2}+\frac{4\tau_C}{1+(2\omega_D\tau_C)^2}\right] \quad (5)$$

where $(2\pi\Delta e^2Qq/h)^2$ is Q_0, the quadrupole coupling constant, η the asymmetry parameter of the motion, ω_Q the angular resonance frequency of ^{2}H at the given field strength, and τ_C the correlation time of the motion. The T_1 and τ_C values of the two B1 and B2 patterns at different temperatures are summarized in Table 5.

On the assumption of the Arrhenius relation and Boltzmann distribution for the temperature dependence of the correlation times, the experimental energetic barriers for the in-plane B1 and the out-of-plane B2 motions have been calculated by using eq 4 and found equal to 8.4 and 11.4 kJ/mol, respectively. The agreement between the calculated and experimental values for B1 is excellent whereas the discrepancy of 3 orders of magnitude found for B2 could be explained considering that this complex motion includes a slow out-of-plane reorientation and a fast in-plane reorientation, where the latter is in the same time scale of B1. The experimental evaluation of T_1 values by NMR methods provides weighted average values accounting for the different relaxation mechanisms.[24] The presence of the fastest in-plane reorientation in both B1 and B2 leads to comparable values of T_1 and of the energetic barrier.

It is noteworthy that ^{2}H NMR spectra with a line shape very similar to that of Figure 8c have been observed for benzene-d_6 molecules in $[NMe_4][Cd_3(CN)_7]\cdot 1.5C_6D_6$:[14c] in that case two kinds of guest molecules are clathrated in the voids of the crystalline compound, whose location was definitively assessed by X-ray analysis. One molecule undergoes the ordinary in-plane rotational motion B1, while the other one, in a looser packing, is involved in a precessional motion (nutation) of the C_6 axis in a cone angle of 36.9°. It is noteworthy the activation energy of 47(8) kJ mol^{-1} estimated for the latter motion[14c] is very close to the one found for the out-of-plane motion in **2** by MD calculations (see above).

Analogously, it can be assumed that the two types of guest molecules exhibiting different dynamics can be detected inside the capsule: one molecule can be constrained in the axially symmetric motion B1, while the other one can be in the mobile state B2 and the two states are in the slow exchange regime in the ^{2}H NMR time scale ($\tau_C < 10^{-4}$ s). Therefore, by comparison with the MD simulations data it can be concluded that the motion B1 can be associated to the state S1 where the inward inclined wall constrains the benzene guest in a parallel in-plane reorientation with an eventual wobbling of the benzene ring in a small cone angle. Analogously, the motion B2 can be associated with the state S2 where an out-of-plane complete reorientation becomes possible due to the wider space available for the benzene wobbling in a larger cone angle.

Assuming that the two motions B1 and B2 are in the fast regime region and in the slow exchange, integration of the two patterns leads to the average populations of the two states B1 and B2 given in Table 4. It is worth noting that they are about equal at room temperature but the inner ^{2}H pattern becomes prevalent by increasing the temperature: an intensity ratio of 2:1 in favor of the latter was actually found at 373 K. Thermogravimetric analysis of capsule **2** evidenced that about 40% of the guest molecules, corresponding to a 2% w/w of the total mass, escaped from the cavity after the thermal treatment. FT-IR analysis of the heated capsule **2** ruled out their partial or total decomposition. Indeed, the imide N−H stretching of the cavitand moieties at 3332 cm^{-1} indicates that the two halves are still joined via hydrogen bonding and the capsules are integer (Figure 10).[4b] When the ^{2}H NMR spectrum of the thermally treated capsule **2** was recorded at room temperature, the resulting ^{2}H NMR inner pattern of Figure 8b slightly changed in intensity. In particular the area of this ^{2}H signal is still comparable to that observed in the ^{2}H NMR spectrum at 373 K (Figure 8c). It is worth noting that when the heated capsules were exposed to a benzene-d_6 stream they uptake one additional guest molecule and the double occupancy of the cavity is newly reestablished. The ^{2}H NMR spectrum of the capsules after the latter treatment exhibits the expected 1:1 intensity ratio of the two Pake patterns. This suggests that the relative intensity of the inner ^{2}H NMR pattern at 373 K accounts for two contributions: the one resulting from the benzene-d_6 guest involved in B2 motion and

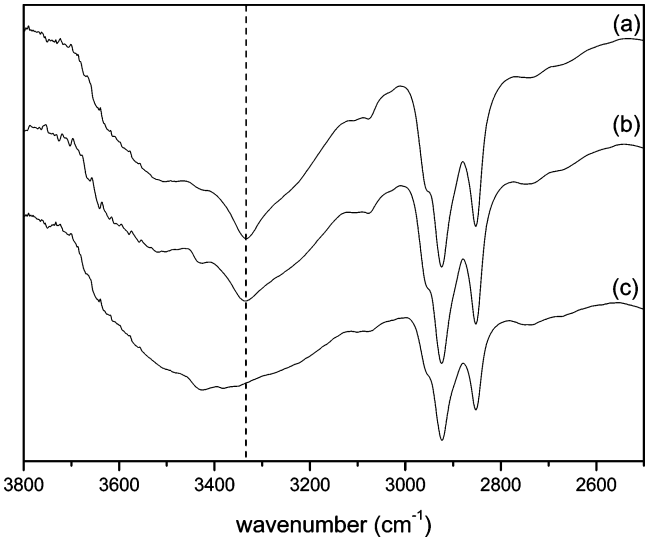

Figure 10. Infrared spectra in the wavenumber range 3800−2500 cm^{-1} of powder benzene-d_6-filled capsule 2: (a) as prepared; (b) after treatment at 373 K for 2 h; and (c) after heating, with a rate of 10 deg/min, up to 523 K. The dashed line at 3332 cm^{-1} indicates the position of the broad imide N−H stretching absorption of the H-bonded capsule[4b] and clearly demonstrates the stability of **2** up to 373 K.

the other one from the capsule showing the single occupancy of inner space. Unfortunately, we are unable to discriminate between the two contributions due to the similarity of the two line shapes.

Conclusions

In the present study the reorientational dynamics of benzene inside the cavitand-based self-assembled capsule **1·1** has been studied by combining MD simulations and temperature-dependent solid-state ^{2}H NMR spectroscopy.

A reduced mobility of the guest inside the cavity has been clearly demonstrated. In particular, a fast complete reorientation around the C_6 symmetry axis of the benzene molecules, with correlation times of the order of picoseconds, was evidenced by MD calculations and by ^{2}H NMR spectroscopic analysis as well. A low activation energy was calculated for this motion, which is comparable to that found for liquid benzene.

In contrast, the out-of-plane reorientation is characterized by correlation times of the order of nanoseconds in the range 293−373 K and microseconds below 293 K, with an activation energy almost four times the value of liquid benzene. This reorientation occurs only for a fraction of the guest molecules and is characterized by a precessional motion (nutation) of the C_6 symmetry axis predicted by both MD and ^{2}H NMR line-shape simulations.

The in-plane reorientation easily occurs in less symmetrical capsules with one inward inclined wall and with the benzene plane parallel to it. The out-of-plane reorientation process requires the re-opening of the inclined wall to give a more symmetrical capsule with a larger space available.

This study shows how the combination of MD simulations with ^{2}H NMR spectroscopy allows a straightforward attribution of the ^{2}H NMR line shape and definition of the kind of motions and of the corresponding time scale and activation barriers of guest molecules inside cavitands.

This approach discloses the possibility of an in-depth investigation of the complex phenomena involved in the dynamics of host−guest complexes and more in general on the complementarity between simulation and experiments for the clarification of complex physicochemical processes.

Acknowledgment. We gratefully acknowledge Dr. Patrizia Oliva for collaboration in recording the ^{2}H NMR spectra.

References and Notes

(1) (a) Rebek, J., Jr. *Acc. Chem. Res.* **1999**, *32*, 278. (b) Hof, F.; Craig, S. L.; Nuckolls, C.; Rebek, J., Jr. *Angew. Chem., Int. Ed.* **2002**, *41*, 1488. (c) Rebek, J., Jr. *Angew. Chem., Int. Ed.* **2005**, *44*, 2068.

(2) (a) Wyler, R.; de Mendoza, J.; Rebek, J., Jr. *Angew. Chem., Int. Ed. Engl.* **1993**, *32*, 1699. (b) Branda, N.; Wyler, R.; Rebek, J., Jr. *Science* **1994**, *263*, 1222. (c) Meissner, R.; Rebek, J., Jr.; de Mendoza, J. *Science* **1995**, *270*, 1485.

(3) (a) Rudkevich, D. M. In *Calixarenes 2001*; Asfari, Z., Böhmer, V., Harrowfield, J., Vicens, J., Eds.; Kluwer Academic Publishers: Dordrecht, The Netherlands, 2001; pp 155−180. (b) Vysotsky, M. O.; Thondorf, I.; Böhmer, V. *Angew. Chem., Int. Ed.* **2000**, *39*, 1264.

(4) (a) MacGillivray, L. R.; Atwood, J. L. *Nature* **1997**, *389*, 469−472. (b) Heinz, T.; Rudkevich, D. M.; Rebek, J., Jr. *Nature* **1998**, *394*, 764.

(5) (a) Körner, S. K.; Tucci, F. C.; Rudkevich, D. M.; Heinz, T.; Rebek, J., Jr. *Chem. Eur. J.* **2000**, *6*, 187−195. (b) Scarso, A.; Onagi, H.; Rebek, J., Jr. *J. Am. Chem. Soc.* **2004**, *126*, 12728−12729.

(6) Hayashida, O.; Sebo, L.; Rebek, J., Jr. *J. Org. Chem.* **2002**, *67*, 8291.

(7) (a) Scarso, A.; Trembleau, L.; Rebek, J., Jr. *Angew. Chem., Int. Ed.* **2003**, *42*, 5499. (b) Scarso, A.; Trembleau, L.; Rebek, J., Jr. *J. Am. Chem. Soc.* **2004**, *126*, 13512−13518.

(8) Shivanyuk, A.; Scarso, A.; Rebek, J., Jr. *Chem. Commun.* **2003**, 1230.

(9) Scarso, A.; Shivanyuk, A.; Hayashida, O.; Rebek, J., Jr. *J. Am. Chem. Soc.* **2003**, *125*, 6239.

(10) Rechavi, D.; Scarso, A.; Rebek, J., Jr. *J. Am. Chem. Soc.* **2004**, *126*, 7738.

(11) (a) Shivanyuk, A.; Rebek, J., Jr. *J. Am. Chem. Soc.* **2002**, *124*, 12074. (b) Shivanyuk, A.; Rebek, J., Jr. *Angew. Chem., Int. Ed.* **2003**, *42*, 684.

(12) Chen, J.; Rebek, J., Jr. *Org. Lett.* **2002**, *4*, 327.

(13) Fyfe, C. A. *Solid State NMR for Chemists*; C.F.C. Press: Guelph, Ontario, 1983.

(14) (a) Brouwer, E. B.; Enright, G. D.; Ripmeester, J. A. *J. Am. Chem. Soc.* **1997**, *119*, 5404. (b) Zaborowski, E.; Zimmermann, H.; Vega, S. *J. Am. Chem. Soc.* **1998**, *120*, 8113. (c) Nishikiori, S.; Kitazawa, T.; Kim, C. H.; Iwamoto, T. *J. Phys. Chem. A* **2000**, *104*, 2591. (d) Trezza, E.; Grassi, A. *Macromol. Rapid Commun.* **2002**, *23*, 260. (e) Albunia, A. R.; Graf, R.; Guerra, G.; Spiess, H. W. *Macromol. Chem. Phys.* **2005**, *206*, 715. (f) Medick, P.; Vogel, M.; Rössler, E. *J. Magn. Reson.* **2002**, *159*, 126. (g) Kustanovich, I.; Vieth, H. M.; Luz, Z.; Vega, S. *J. Phys. Chem.* **1989**, *93*, 7427. (h) Van Wagenigen, A. M. A.; Verboom, W.; Zhu, X.; Ripmeester, J. A.; Reinhoudt, D. N. *Supramol. Chem.* **1998**, *9*, 31. (i) Chopra, N.; Chapman, R. G.; Chuang, Y.; Sherman, J. C.; Burnell, E. E.; Polson, J. M. *J. Chem. Soc., Faraday Trans.* **1995**, *91*, 4127. (j) Xiong, J.; Maciel, G. E. *J. Phys. Chem. B* **1999**, *103*, 5543.

(15) Müller-Plathe, F. *Macromolecules* **1996**, *29*, 4782.

(16) Witt, R.; Sturz, L.; Dolle, A.; Müller-Plathe, F. *J. Phys. Chem. A* **2000**, *104*, 5716.

(17) Müller-Plathe, F. *Comput. Phys. Commun.* **1993**, *78*, 77.

(18) Berendsen, H. J. C.; Postma, J.; van Gunsteren, W.; Di Nola, A.; Haak, J. *J. Chem. Phys.* **1984**, *81*, 3684.

(19) Allen, M. P.; Tildesley, D. J. *Computer Simulation of Liquids*; Clarendon Press: Oxford, UK, 1987.

(20) Ferro, R.; Tedesco, C.; Gaeta, C.; Neri, P. *J. Inclusion Phenom. Macrocyclic Chem.* **2005**, *52*, 85.

(21) Jorgensen, W. L.; Severance D. *J. Am. Chem. Soc.* **1990**, *112*, 4768.

(22) Milano, G.; Müller-Plathe, F. *J. Phys. Chem. B* **2004**, *108*, 7415.

(23) Macho, V.; Brombacher, L.; Spiess, H. W. *Appl. Magn. Reson.* **2001**, *20*, 405. The NMR-WEBLAB program is freely accessible at the following WEB page: http://www.mpip-mainz.mpg.de/weblab41/.

(24) Claridge, T. D. W. *High-Resolution NMR Techniques in Organic Chemistry*; Pergamon Press: Oxford, UK, 1999; pp 25−35.

(25) Abragam, A. *Principles of Nuclear Magnetism*; Clarendom Press: Oxford, UK, 1985; p 314.